Isolation and characterization of bacteriophages against IMP-6-producing *Klebsiella pneumoniae* isolated from clinical settings in Japan

Kohei Kondo[a], Satoshi Nakano[a], Junzo Hisatsune[a], Yo Sugawara, Michiyo Kataoka[b], Shizuo Kayama[a], Motoyuki Sugai[a], Mitsuoki Kawano[c]#

[a]Antimicrobial Resistance Research Center, National Institute of Infectious Diseases, Higashimurayama, Tokyo, Japan

[b]Department of Pathology, National Institute of Infectious Diseases, Toyama, Shinjuku-ku, Tokyo, Japan

[c]Department of Nutritional Sciences, Nakamura Gakuen University, Jonan-Ku, Fukuoka, Japan

Notes: Kohei Kondo and Mitsuoki Kawano contributed equally to this work.

Running Head: Phages infecting $bla_{\text{IMP-6}}$-harboring *K. pneumoniae*

#Address correspondence to Mitsuoki Kawano, mkawano@nakamura-u.ac.jp

Abstract

Carbapenemase-producing *Enterobacteriaceae* (CPE) are one of the most detrimental species of antibiotic-resistant bacteria worldwide. Phage therapy has emerged as an effective strategy for the treatment of infections caused by CPE pathogens. In west Japan, the increasing occurrence of *Klebsiella pneumoniae* harboring the pKPI-6 plasmid, which encodes $bla_{\text{IMP-6}}$, is a growing concern. To manage such major antimicrobial-resistant pathogens, we isolated 29 novel phages from sewage in Japan, targeting 31 strains of *K. pneumoniae* and one strain of *Escherichia coli* harboring the pKPI-6 plasmid. Electron microscopy analysis indicated that of the 29 isolated phages, 21 (72.4%), 5 (17.2%), and 3 (10.3%) belonged to *Myoviridae*, *Siphoviridae*, and *Podoviridae*, respectively. Host range analysis revealed that 20 *Myoviridae* members in isolated phages infected 25–26 strains of *K. pneumoniae*, indicating that most of the isolated phages have a broad host range. The *K. pneumoniae* Kp21 can only be infected by phage øKp_21, while Kp22 can be infected by more than 20 phages. We applied a phage cocktail, which consists of 10 phages, against Kp21 and Kp22 and found that the phage cocktail delayed the emergence of phage-resistant bacteria for Kp21 strain but not for the Kp22 strain. Furthermore, phage-resistant Kp21 (Kp21r) became prone to be infected from other bacteriophages as a “trade-off” of

35 resistance to phage øKp_21. Our proposed phage set has an adequate number of phages to
36 combat the *K. pneumoniae* strain isolated in Japan. Notably, our work demonstrates how a
37 suitable phage cocktail diminishes the occurrence of phage-resistant bacteria.
38
39 **Importance**
40 *Klebsiella pneumoniae* harboring the plasmid carrying $bla_{\text{IMP-6}}$ is becoming an increasingly
41 hazardous species in Japan. We collected and characterized 29 novel bacteriophages that
42 infect *K. pneumoniae* carrying the pKPI-6 plasmid, isolated in clinical settings of west
43 Japan. Our phages showed broad host ranges. We applied a phage cocktail treatment
44 constructed from 10 phages against two host strains, Kp21 and Kp22, which show different
45 phage susceptibility patterns each other. Although the phage cocktail delayed phage-
46 resistant Kp21 emergence, the emergence of phage-resistant Kp22 could not be delayed.
47 Moreover, phage-resistant Kp21 became sensitive to other phages, which did not originally
48 infect wild-type Kp21. Our study demonstrates how a suitable phage cocktail can diminish
49 the occurrence of phage-resistant bacteria.
50
51

Introduction

Carbapenemase-producing *Enterobacteriaceae* (CPE) are high-risk bacteria in clinical settings globally. *Klebsiella pneumoniae*, a member of the family *Enterobacteriaceae*, causes nosocomial infections and is one of the most common causes of life-threatening infections caused by multidrug-resistant bacteria worldwide (1). bla_{IMP} genes are classified as class B metallo-β-lactamases. $bla_{\mathrm{IMP\text{-}1}}$ and $bla_{\mathrm{IMP\text{-}6}}$ genes are predominantly detected in CPE isolated from Japan (2, 3), whereas other types of carbapenemases (NDM, KPC, and OXA-48) are mainly detected in CPE isolated from other countries (4). *Klebsiella pneumoniae* with the pKPI-6 plasmid encoding $bla_{\mathrm{IMP\text{-}6}}$ (5), which is susceptible to imipenem but resistant to meropenem, has become increasingly common in clinical settings in west Japan since their emergence in 2009 (6). These strains are therefore of major concern in clinical settings because of the inappropriate selection of antibiotics for treatment.

Recently, research on the use of bacteriophages as an alternative for the treatment of infections caused by antimicrobial-resistant bacteria has become increasingly prevalent (7). Phage therapy targeting *Staphylococcus aureus* (8) and *Mycobacterium tuberculosis* (9) has been administered successfully to patients. Furthermore, a recent study has demonstrated

69 effective phage therapy targeting CPE in clinical settings (10). Thus, phage therapy is now
70 recognized as a highly reliable strategy to combat nosocomial pathogens.
71 Following the use of phages against bacteria, phage-resistant bacteria have emerged (11)
72 *in vitro* (12) and *in vivo* (13). The phage cocktail strategy, which consists of several types
73 of phages, is often used to prevent the emergence of phage-resistant bacteria. A phage bank
74 is useful to quickly apply the phage cocktail in clinical settings (14), especially in
75 emergency cases. As national phage banks are pertinent for the instant management of
76 contingent nosocomial pathogen outbreaks, several countries have constructed public phage
77 banks for the efficient use of phage therapy (14, 15). However, there is no public phage
78 bank optimized for the trend of antibiotic-resistant bacteria in Japan.
79 In this study, we isolated and characterized 29 bacteriophages targeting IMP-6-producing *K.*
80 *pneumoniae* and *Escherichia coli* clinical isolates as the first step in constructing a public
81 phage library in Japan. We also describe the mechanisms by which phage cocktails reduce
82 the emergence of phage-resistant *K. pneumoniae.*
83
84
85

Results

1. Phage hunting and morphological analysis of novel bacteriophages

We performed phage hunting from the sewage system in west Japan, which yielded 29 phages against 32 *K. pneumoniae* and one against *E. coli* (Ec1) isolates harboring pKPI-6. Each phage name number indicates the corresponding host number. For instance, øEc_1 and øKp_1 phages were isolated from *E. coli* Ec1 and *K. pneumoniae* Kp1, respectively, as their corresponding hosts. All phage-corresponding hosts combinations are listed in Table S1. We did not discover appropriate phages against *K. pneumoniae* (Kp2, Kp6, Kp25, Kp28, and Kp29). Morphological analysis using electron microscopy indicated that 21/29 (72.4 %) isolated phages belonged to *Myoviridae*, 5/29 (17.2 %) belonged to *Siphoviridae*, and 3/29 (10.3 %) belonged to *Podoviridae* (Fig. 1). All TEM images of *Myoviridae* were shown in Fig. S1 The transmission electron microscopy image strongly suggested that øEc_1 belonged to *Podoviridae* and C3 morphotype (honeycomb-like) phages (16–18), which possess an elongated head (height, 136.6 nm ± 1.8 nm; width, 61.7 nm ± 3.6 nm; tail, 15.8 nm ± 2.3 nm) (Fig. 1). øEc_1 formed turbid plaques on the *E. coli* Ec1 strain. øKp_21 was classified as *Myoviridae* (height, 133.8 nm ± 3.1 nm; width, 137.1 nm ± 1.1 nm; tail,

109.7 nm ± 1.0 nm) (Fig. 1). Furthermore, øKp_21 had a branched tail (tail spike) fiber and formed clear plaques on the lawn of *K. pneumoniae* Kp21.

2. Host range determination and analysis of the correlation between plaque size and efficiency of plating (EOP)

We next determined the host range and its EOP for all phage–host combinations (Fig. 2) (Table S2). We selected two standard strains (ATCC BAA 1705, ATCC BAA 1706) as the control for *K. pneumoniae*. Although no novel phages against five hosts (Kp2, Kp6, Kp25, Kp28, and Kp29) were isolated, the host range experiment indicated that several isolated phages formed plaques against Kp2, Kp6, Kp25, and Kp29 but not Kp28 (Fig. 2). Phages øKp_8 and øKp_17 showed the broadest host range (26/32 *K. pneumoniae* host strains). Most phages (øKp _3, øKp _5, øKp _9, øKp _10, øKp _12, øKp _13, øKp _15, øKp _16, øKp _18, øKp _19, øKp _20, and øKp _26) showed plaque formation on 25 host *K. pneumoniae* strains, indicating that these phages have a broad host range (infecting ≧ 25 host strains). In contrast, several phages showed a narrow host range (infecting ≦ 4 host strains). For example, øKp_31 infects Kp15, Kp17, Kp26, and Kp31. øKp_27 (*Siphoviridae*), øKp_30 (*Podoviridae*), and øKp_32 (*Myoviridae*) infect only Kp27, Kp30,

and Kp32, respectively (Fig. 2). Overall, our phage set can handle the *K. pneumoniae* isolated in clinical settings and has an adequate number of phage types to construct a phage cocktail against *K. pneumoniae* in this study.

We observed that high EOP values indicated the formation of large plaques. Thus, we performed correlation analysis between EOP values and plaque size of eight representative phages that showed different host range pattern. Pearson's correlation coefficients (R values) were 0.75 for øKp_1, 0.86 for øKp_7-1, 0.70 for 7-2, 0.55 for øKp_14, 0.25 for øKp_21, 0.80 for øKp_24, 0.83 for øKp_27, and 0.65 for øKp_31 (Fig. S2). Therefore, plaque size was positively correlated with the EOP.

3. OD_{600} kinetics of *K. pneumoniae* challenged with phages

OD_{600} kinetics were analyzed for all phage–indicator host combinations. Individual phages were added to cultures of indicator hosts at 10^8 pfu/ml. The OD_{600} decreased 1 h after each phage was added, while that of the Ec1 and øEc_1 mixture did not decrease and approximated that of the host strain without any phages (Fig. 3). The OD_{600} in all phage combinations increased again 6–10 h after the addition of each phage. This result indicates that phage-resistant bacteria emerged in almost all the phage–host combinations.

136

137 **4. Cocktail analysis of phage-resistant bacteria Kp21**

138 Kp21 can only be infected by øKp_21, while Kp22 can be infected by 23 phages (Fig. 2).
139 Furthermore, øKp_21 infects 18 hosts including Kp21, but øKp_22 infects Kp22 and Kp31
140 strains only (Fig. 2). We focused on these contrasting strains, øKp_21 and øKp_22, for the
141 phage cocktail experiment. The phage cocktail consisted of 10 phages (øKp_16–26), which
142 include 8 *Tevenviridae*, 1 *Alcyoneusvirus*, and 1 *Siphoviridae*. In the Kp21 and øKp_21
143 combination, the OD_{600} increased again after 6 h and reached that of the negative control
144 after 24 h (Fig. 4A). However, the OD_{600} did not increase until 14 h when Kp21 was
145 combined with the phage cocktail (Fig. 4A). Therefore, the phage cocktail delayed the
146 emergence of phage-resistant Kp21 in the *in vitro* assay. However, the OD_{600} of the cocktail
147 against Kp22 increased again after 10 h, which is the same time taken as the OD_{600} of
148 single øKp_22 (Fig. 4C). This result indicates that the phage cocktail failed to delay the
149 emergence of phage-resistant Kp22. We isolated øKp_21-resistant Kp21 (Kp21r) and
150 øKp_22-resistant Kp22 (Kp22r) according to the method described in the Materials and
151 methods section. Although the OD_{600} kinetics in the mixture of Kp21r and øKp_21 did not
152 decrease and approximated that of Kp21r without any phages, the OD_{600} reduced in the

153 Kp21r–phage cocktail combination (Fig. 4B). This result indicates that the Kp21r strain is
154 resistant to phage 21 but susceptible to the phage cocktail. However, OD_{600} did not
155 decrease in either Kp22r-øKp_22 or Kp22r-cocktail combinations, suggesting that the
156 phage-resistant Kp22r is not susceptible to either øKp_22 or the phage cocktail (Fig. 4D).
157

158 **5. Shifting of phage sensitivity between Kp21 and Kp21r**

159 To analyze the susceptibility of Kp21r to the phage cocktail, we compared phage plaque
160 formation between Kp21 and Kp21r. According to the host range analysis, no phages
161 formed plaques on Kp21. However, the Kp21r strain became susceptible to øKp_16, 17, 18,
162 19, 20, 23, and 26, which are of the genus *Tevenviridae*. This result suggests that Kp21r
163 becomes prone to be infected from other phages in compensation for resistance to øKp21
164 (Fig. 5A). Furthermore, the Kp21r strain showed a sparse background on LB agar plates
165 containing *Tevenviridae* viruses (Fig. 5A). This sparse background is not caused by
166 confluent plaque lysis. This implies a mechanism by which the phage cocktail prevents the
167 emergence of phage-resistant bacteria without phage infection. To determine the efficiency
168 with which phages can kill the Kp21r strain, we measured the colony-forming unit (cfu)
169 values of Kp21 and Kp21r by mixing the individual phages used in the phage cocktail. In

øKp_21, the cfu of Kp21 was reduced (10^4 cfu/ml), but that of Kp21r was almost the same as that of the control Kp21r (10^7–10^8 cfu/ml). In øKp_22 and øKp_24, cfu/ml in Kp21r was not significantly decreased compared to that in Kp21. These results are consistent with our observation that these phages are incapable of infecting Kp21 and Kp21r. In other phages, the cfu of Kp21r strain significantly decreased compared to that of Kp21. In particular, colonies were not detected for øKp_18, 19, 20, or 23-Kp21r combinations. Our results indicate that Kp21r viable cells were wiped out by phages that newly infected Kp21r.

6. Characterization of Kp21 and Kp21r

To analyze the differences between the strains Kp21 and Kp21r, we performed an adsorption assay of øKp_21 for Kp21 and Kp21r. The assay showed that unadsorbed øKp_21 for the Kp21r strain was approximately 100 % at 5 min after the phage was added to the Kp21 strain, while for Kp21, the value was 2–5 % (Fig. 6A). In addition, no plaques were detected when øKp_21 was input at 10^9 pfu (EOP < 10^{-9}) (Fig. 6B). These results indicate that øKp_21 loses its ability to adsorb Kp21r. Next, we detected single nucleotide polymorphism (SNPs) between Kp21 and Kp21r. Insertion mutations were detected in two genes, *thpA* (encoding the inner membrane protein) and *cpsA* (encoding exopolysaccharide

187 synthesis genes) as shown in Table S4; this result suggests that the øKp_21 phage
188 recognizes the capsular polysaccharide of Kp21. Insertion mutations of *cpsA* in Kp21r
189 occur at the 452nd nucleotide position and a stop codon appeared at the 463rd nucleotide
190 position (Fig. 6C). Therefore, 141 amino acids are truncated at C-terminus CpsA of Kp21r
191 (154 amino acids long); the wild-type CpsA amino acid length is 295. This severe
192 truncation can result in deficient capsular polysaccharide biosynthesis of Kp21r.
193
194 **Discussion**
195 Phage therapy is increasingly being recognized as an effective strategy to combat
196 antimicrobial-resistant bacteria, especially nosocomial pathogens (8–10, 19). A recent study
197 demonstrated that inflammation in a mouse model of inflammatory bowel disease (IBD)
198 was suppressed by the eradication of *K. pneumoniae* using a phage cocktail. This suggests
199 that phage therapy targeting *K. pneumoniae* successfully treats IBD in humans (20).
200 In this study, we isolated and characterized novel bacteriophages targeting antimicrobial-
201 resistant *K. pneumoniae* harboring the pKPI-6 plasmid, which encodes $bla_{\text{IMP-6}}$. We isolated
202 29 novel phages from sewage in west Japan against the *K. pneumoniae* and *E. coli*
203 harboring pKPI-6 plasmid. Genome sequence analysis suggests that *Tevenviridae* members

in this study except øKp_22 are very similar in genome size and identity; thus, these phages were considered to be variants of the same species (Table S1). We were concerned that our phages encode antimicrobial resistance (AMR) and virulence factor (VF) genes, because phages can transfer these genes in clinical settings (21–23). However, our analysis indicated that neither AMR nor VF genes were detected in isolated phage genomes, thereby allowing the application of these phages in clinical settings.

Our host range experiment analysis showed that most of the phages, which were classified as *Myoviridae*, formed plaques on the 25 *K. pneumoniae* strains. Specific host strains (*K. pneumoniae* Kp12 to Kp20) showed higher EOP (Fig. 3) against most phages, suggesting that several strains exhibit high susceptibility to novel phages isolated from west Japan. Moreover, host range experiment results indicated that EOP and plaque size are positively correlated in several phages such as øKp_1, 7, 7-1, 14, 24, 27, and 31. To the best of our knowledge, few reports have described the correlation of these factors (24); however, we hypothesize that phages that show a larger plaque size have a greater burst size and/or adsorption efficacy. These results can facilitate the development of novel phages that have a higher virulence to the host bacteria; moreover, our work can also guide the selection of phage strains for developing a phage cocktail (25, 26).

The phage cocktail experiment revealed that Kp21r became newly susceptible to other phages in the phage cocktail. Phage cocktail analysis showed that Kp22 did not retard the emergence of phage-resistant Kp22 (Kp22r), which was in contrast to the results for the Kp21 strain. This antithetical result of the Kp21 and Kp22 cocktail experiment implies that the phage cocktail is not an all-round strategy; however, it remains the most reliable strategy to combat bacteriophages, thus far. No universal methods or guidelines have been established for developing the cocktail, and it is difficult to predict the combination of phages that can inhibit the emergence of phage-resistant bacteria with the greatest efficiency. However, it has been reported that several phages that recognize different receptors of the host should be mixed to efficiently decrease the occurrence of phage-resistant bacteria (27–29).

Our experimental results indicate that Kp21r became infected by øKp_16, 17, 18, 19, 20, 23, and 26, while Kp21 was only subject to infection by øKp_21 (Fig. 5). This result suggests that phage–resistant bacteria is easily attacked by other phages that exist in environment during evolutionary arms race. Adsorption assays explained that øKp_21 lacks the ability to adsorb Kp21r. SNP analysis of Kp21 and Kp21r revealed that insertion mutations occurred in at least two genes; *cpsA*, encoding putative capsular biosynthesis

protein and *thpA*, encoding sugar ABC transporter substrate-binding protein. It has been reported that capsular polysaccharide function as the barrier to infect phages (30). A recent article reports a novel phage that recognizes the capsular polysaccharide of *K. pneumoniae* (31), and accordingly, we speculate that capsular polysaccharide is one of the factors allowing øKp_21 to adsorb to its host Kp21. We found that *Myoviridae*, in the phage cocktail, diminished the lawn density of Kp21r on the plates. We posit that this phenomenon was caused by lysis mechanisms such as "lysis from without (LO)" or "rapid lysis" (32, 33). Gp5 in T4 phage, which encodes tail lysozyme, is known to cause LO (34). Gp5 forms the complex with T4 phage tail and when T4 phage adsorbs to their host, Gp5 degrades the peptidoglycan layer. We found that members of *Myoviridae*, used for the phage cocktail in this study, encode the baseplate with tail lysozyme (Table S3), which has the capability of peptidoglycan degradation. SNPs analysis of Kp21 and Kp21r suggests that Kp21r possesses deficient capsular polysaccharide, and thus, phage tail protein encoded in *Myoviridae* may more efficiently degrade Kp21r peptidoglycan and result in rapid lysis. Some studies have reported that phage-resistant bacteria become susceptible to antibiotic due to mutation in the genes involved in antibiotics resistance and showed that phages and antibiotics combination effectively kills the target bacteria (35–38). Our results

255 demonstrate that the combinations of phage and phage-encoded tail lysozyme efficiently
256 eliminate and/or inhibit the phage-resistant bacterial growth (39).

257 In conclusion, we isolated and characterized novel phages infecting *K. pneumoniae* and *E.*
258 *coli* harboring the pKPI-6 plasmid; this is the first step in the construction of a public phage
259 bank and phage therapy in Japan. Overall, our phage sets can diminish the threat of *K.*
260 *pneumoniae* harboring the pKPI-6 plasmid isolated in clinical settings. Our phage sets also
261 contain an adequate number of phage types for developing a phage cocktail. However, the
262 development of a high-throughput method is required for efficiently isolating additional
263 novel phages.

264

265 **Materials and Methods**

266 **1. Phage isolation and host information**

267 Thirty-two IMP-6-producing isolates of *K. pneumoniae* and one IMP-6-producing isolate
268 of *E. coli* were isolated from clinical settings in western Japan. Further, 29 novel phages
269 were isolated from sewage in west Japan. Briefly, 100 µl of sewage was mixed with an
270 overnight culture of the indicator host, and the mixture added to 3 ml of YT-soft agar prior
271 to inoculation onto Luria–Bertani (LB) agar. The plates were incubated at 37°C overnight,

and thereafter, single-plaque isolation was performed. Plaques were suspended in 1 ml LB medium and incubated for 2 h. Next, 50 µl chloroform (Fujifilm Wako Pure Chemical Corporation, Osaka, Japan) was added to each solution; the mixture was vortexed and then centrifuged at 10,000 ×*g* for 10 min at 4°C. Supernatants and individual indicator hosts were mixed and incubated at 37°C overnight on LB agar plates. The single-plaque isolation procedure was repeated three times, and isolated phages were stored at 4°C until use. Kp21 was renamed from the *K. pneumoniae* f22 strain.

2. Phage propagation and purification

Pre-cultured host strains were inoculated into 3 ml fresh LB medium (1:100) and incubated at 37°C until the OD_{600} reached 0.5. Thereafter, each phage that was originally isolated using the indicated host was added and incubated at 37°C with shaking at 200 rpm for 4–6 h. Following lysis, 50 µl chloroform (FUJIFILM Wako Pure Chemical Corporation) was added to 1 ml of the phage lysate, vortexed, and then centrifuged at 9,100 ×*g* for 10 min. Supernatants were filtered using a 0.22 µm pore-size membrane (Millipore, MA, USA). Cesium chloride (CsCl) density gradient phage purification was performed as described previously (40, 41) with some modification. Briefly, 10% polyethylene glycol

289 6000 (FUJIFILM Wako Pure Chemical Corporation) and 0.5 M NaCl were added to phage
290 lysates and kept at 4°C for 1.5 h. Thereafter, phage lysates were centrifuged at 10,000 ×*g*
291 for 30 min. Phage pellets were suspended in 1 ml TM buffer (10 mM Tris-HCl, and 5 mM
292 $MgCl_2$ [pH 7.5]), and 100 µg/ml DNase I (Roche, Basel, Switzerland) and RNase I
293 (Thermo Fisher Scientific, MA, USA) were added to the phage solution and incubated at
294 37°C for 30 min. CsCl (FUJIFILM Wako Pure Chemical Corporation) at three different
295 weights (ρ = 1.3, 1.5, and 1.7) and phage solution were overlaid in tubes and
296 ultracentrifuged (Optima MAX-TL; Beckman Coulter, California, USA) at 100,000 ×*g* for
297 1 h. Phage bands were then collected and dialyzed in SM buffer (25 mM Tris-HCl [pH, 7.5],
298 100 mM NaCl, and 8 mM $MgSO_4$).
299

300 **3. Phage propagation and electron microscopic imaging**

301 Copper mesh grids coated with formvar and carbon (Veco grids; Nissin EM, Tokyo,
302 Japan) were glow-discharged and placed on drops of the phages for 1 min. Thereafter, they
303 were rinsed with distilled water and stained with a 2% uranyl acetate solution. Samples
304 were examined using transmission electron microscopy (HT7700; Hitachi Ltd., Tokyo,
305 Japan) at 80 kV.

306

307 **4. Host range determination and EOP assay**

308 Each host was incubated at 37°C overnight, and 100 µl of each overnight culture was
309 mixed with 100 µl of each phage. Thereafter, 5 ml of 0.6 % soft agar was added to the
310 host–phage mixture and inoculated onto LB agar. The plates were then incubated at 37°C
311 overnight, and the number of plaques in each plate counted. EOP was calculated using the
312 formula below:

313 EOP = plaques of individual phage and host combination/plaques of indicator host and
314 phage combination.

315 The detection limit of EOP was set as 10^{-4} pfu. EOP was measured for all phage–bacteria
316 combinations. Each plaque image was taken using scan1200 (Interscience, Montpellier,
317 France) for measuring plaque sizes. Plaque size (mm^2) was measured using Fiji
318 (https://fiji.sc) version 2.3.0, with 1 mm being 11 pixels. For very small plaques, the edge
319 of individual plaques was detected using the "find edge" tool in Fiji. Ten plaque areas were
320 measured in each phage–host combination if the number of plaques on the plate was more
321 than 10.

322

5. OD_{600} kinetics and cocktail experiment

The host colony was pre-cultured in LB medium overnight at 37°C. Subsequently, the pre-cultured bacteria were inoculated (1:100) into fresh LB medium and incubated at 37°C with shaking at 200 rpm until OD_{600} = 0.1. Each indicated phage was added to the culture at 1.0 × 10^8 pfu/ml and the mixed culture incubated at 37°C with shaking at 200 rpm. OD_{600} was measured at appropriate times for 24 h. In phage cocktail experiments, 10 phages (øKp_16, 17, 18, 19, 20, 21, 22, 23, 24, and 26) were mixed at 1.0 × 10^7 pfu/ml of each individual phage. All experiments in this section were performed in triplicate.

6. Host and phage genome sequences

All phage genomic DNA was extracted using Norgen phage DNA isolation kit (Norgen Biotak, Birmingham, UK) following the manufacturer's instructions. Each phage DNA library was constructed using the QIA seq FX DNA library kit (Qiagen), and sequencing was performed using the Illumina MiSeq platform. Genome assembly was performed using Shovill with default settings. Phage contigs were filtered with the contig length < 200 and coverage < 25. Bacteria strains and phage strains were annotated using prokka (42) or PGAP (43) version 2021-07-01.build5508. For Nanopore long-read sequencing, we used

the Monarch HMW DNA Extraction Kit for Tissue (NEB, MA, USA) following the manufacturer's instructions.

A long-read library was prepared using the Rapid Barcoding kit (Oxford Nanopore Technologies, Oxford, United Kingdom, catalog number: SQK-RBK004) and sequenced with an R9 flow cell (Oxford Nanopore Technologies, catalog number: FLO-MIN106) and a GridION device (Oxford Nanopore Technologies). Basecalling was performed using Guppy version 5.0.12 with high accuracy mode. The obtained long reads and MiSeq short reads that were trimmed using fastp v0.20.1 were assembled using Unicycler v0.4.8 with default parameters. Annotation was conducted using PGAP version 2021-07-01.build5508.

7. Bioinformatics analysis

For protein prediction in phages, we constructed the phage protein databases from International Committee on Taxonomy of Viruses (ICTV), which consists of 4,312 genomes and 4,62,579 proteins (https://www.ncbi.nlm.nih.gov/genomes/GenomesGroup.cgi?taxid=28883) (September 2021) using local blastp (44) with the e-value threshold < 2e-20. Protein domains were detected using hmmer (https://www.ebi.ac.uk/Tools/hmmer/) with the Pfam-A 35.0

357 database at e-value of < 1e-10. Phage classification was determined according to National
358 Center for Biotechnology Information (NCBI) GenBank and ICTV. Average nucleotide
359 identity was conducted using the average_nucleotide_identity.py program in pyani
360 packages (45). MUMmer was used to align nucleotide sequences. AMR genes and
361 virulence genes were detected using ABRicate version 1.0.1
362 (https://github.com/tseemann/abricate) under default settings. The ResFinder database was
363 used to extract AMR genes (46), and the Virulence Factors Database (VFDB) was used to
364 extract virulence genes (47). The packaging mechanism and terminal repeats were analyzed
365 using Phagetermvirome version 4.0.1 (48), and tRNA was detected using tRNAscan-SE 2.0.
366 (49). Kp21 and Kp21r SNPs analysis was performed using SNIPPY at default settings (50).
367

368 **8. Phage-resistant Kp21 (Kp21r) and Kp22 (Kp22r) strain**

369 Kp21 and Kp22 were cultured with øKp_21or øKp_22, respectively at 37°C. After 24 h of
370 incubation, 1 ml of each culture was centrifuged at 4,400 ×*g* for 10 min. The supernatant
371 was discarded and the pellets washed with LB medium. This procedure was repeated twice.
372 Thereafter, the pellet was resuspended using saline (0.85 % NaCl) and the suspension
373 plated on LB agar and incubated at 37°C overnight. A single colony was incubated

374 overnight at 37°C with shaking at 200 rpm. Glycerol stock of Kp21r culture was stored at –
375 80°C until use.
376
377 **9. Adsorption assay**
378 Kp21 and Kp21r were cultured in LB medium and incubated at 37°C until OD_{600} = 0.5.
379 Subsequently, 3.0×10^6 pfu øKp21 was added and incubated at 37°C with shaking at 200
380 rpm for 5 min. Next, 20 µl chloroform was added to 200 µl of the mixture and vortexed.
381 The samples were then centrifuged at 9,100 ×*g* for 1 min and the supernatant collected. A
382 100 µl aliquot of the supernatant was mixed with Kp21 and plaque assays performed to
383 measure the number of unadsorbed phages. The percentage of the unadsorbed phages was
384 calculated using the formula below:
385 Unadsorbed phage % = the number of phages in supernatant/added phages × 100
386
387 **10. Characterization of switched phage sensitivity between Kp21 and Kp21r**
388 The phage sensitivity of Kp21 and Kp21r were examined. Briefly, 1.0×10^9 pfu of
389 individual phages used in the phage cocktail was mixed with 100 µl of overnight Kp21 or
390 Kp21r culture. Thereafter, 5 ml of 0.6 % soft agar was added to the host and phage mixture

and then poured onto LB agar and incubated at 37°C overnight. The colony count was examined as follows. Kp21 and Kp21r were incubated at 37°C until OD_{600} = 0.1. Subsequently, Kp21 was added to 1.0×10^9 pfu, and the mixture was incubated at 37°C. The mixture was collected 2 h after phages were added and centrifuged at 3,300 ×*g* for 15 min. The supernatant was discarded, and the pellet was suspended in 500 µl phosphate-buffered saline (0.137 M NaCl, 0.27 mM KCl, 0.1 M Na_2HPO_4, 18 mM KH_2PO_4). The suspension was diluted to 10^{-2} and 10^{-4}, and 100 µl of these dilutions was lawned onto LB agar.

11. Data availability

Row sequence reads for all phages were deposited to DDBJ/EMBL/GenBank under Bioproject (number: PRJDB14376), and DRA numbers are listed in Table S1. Complete genome sequences of Kp21 and Kp21r were deposited in GenBank (accession numbers AP026912 and AP026913).

Acknowledgment

This work was partially supported by JSPS KAKENHI (21K1633 to K.K., 18K08455 and 22K08592 to M.K.) from the Ministry of Education, Culture, Sports, Science and Technology (MEXT), Japan; grants (19lm0203008j0003 A058 and 22ym0126811j0001 A255 to M.K.) from the Japan Agency for Medical Research and Development (AMED) and grants (JP21fk0108604j0001, 22fk0108604j0002, 21fk0108132j0002 to M.S.) from Research Program on Emerging and Re-emerging infection Diseases (AMED).

References

1. Effah CY, Sun T, Liu S, Wu Y. 2020. Klebsiella pneumoniae: An increasing threat to public health. Ann Clin Microbiol Antimicrob 19:1–9.

2. Yamagishi T, Matsui M, Sekizuka T, Ito H, Fukusumi M, Uehira T, Tsubokura M, Ogawa Y, Miyamoto A, Nakamori S, Tawa A, Yoshimura T, Yoshida H, Hirokawa H, Suzuki S, Matsui T, Shibayama K, Kuroda M, Oishi K. 2020. A prolonged multispecies outbreak of IMP-6 carbapenemase-producing Enterobacterales due to horizontal transmission of the IncN plasmid. Sci Rep 10:1–9.

3. Abe R, Akeda Y, Sugawara Y, Takeuchi D, Matsumoto Y, Motooka D, Yamamoto N, Kawahara R, Tomono K, Fujino Y, Hamada S. 2020. Characterization of the Plasmidome Encoding

Carbapenemase and Mechanisms for Dissemination of Carbapenem-Resistant Enterobacteriaceae . mSystems 5.

4. Nordmann P, Naas T, Poirel L. 2011. Global spread of carbapenemase producing Enterobacteriaceae. Emerg Infect Dis 17:1791–1798.

5. Kayama S, Shigemoto N, Kuwahara R, Oshima K, Hirakawa H, Hisatsune J, Jové T, Nishio H, Yamasaki K, Wada Y, Ueshimo T, Miura T, Sueda T, Onodera M, Yokozaki M, Hattori M, Ohge H, Sugai M. 2015. Complete nucleotide sequence of the IncN plasmid encoding imp-6 and CTX-M-2 from emerging carbapenem-resistant Enterobacteriaceae in japan. Antimicrob Agents Chemother 59:1356–1359.

6. Shigemoto N, Kuwahara R, Kayama S, Shimizu W, Onodera M, Yokozaki M, Hisatsune J, Kato F, Ohge H, Sugai M. 2012. Emergence in Japan of an imipenem-susceptible, meropenem-resistant Klebsiella pneumoniae carrying bla IMP-6. Diagn Microbiol Infect Dis 72:109–112.

7. Cao F, Wang X, Wang L, Li Z, Che J, Wang L, Li X, Cao Z, Zhang J, Jin L, Xu Y. 2015. Evaluation of the efficacy of a bacteriophage in the treatment of pneumonia induced by multidrug resistance klebsiella pneumoniae in mice. Biomed Res Int 2015.

8. Petrovic Fabijan A, Lin RCY, Ho J, Maddocks S, Ben Zakour NL, Iredell JR, Khalid A, Venturini C, Chard R, Morales S, Sandaradura I, Gilbey T. 2020. Safety of bacteriophage therapy in severe Staphylococcus aureus infection. Nat Microbiol 5:465–472.

9. Dedrick RM, Guerrero-Bustamante CA, Garlena RA, Russell DA, Ford K, Harris K, Gilmour KC, Soothill J, Jacobs-Sera D, Schooley RT, Hatfull GF, Spencer H. 2019. Engineered bacteriophages for treatment of a patient with a disseminated drug-resistant Mycobacterium abscessus. Nat Med 25:730–733.

10. Eskenazi A, Lood C, Wubbolts J, Hites M, Balarjishvili N, Leshkasheli L, Askilashvili L, Kvachadze L, van Noort V, Wagemans J, Jayankura M, Chanishvili N, de Boer M, Nibbering P, Kutateladze M, Lavigne R, Merabishvili M, Pirnay JP. 2022. Combination of pre-adapted bacteriophage therapy and antibiotics for treatment of fracture-related infection due to pandrug-resistant Klebsiella pneumoniae. Nat Commun 13.

11. Oechslin F. 2018. Resistance development to bacteriophages occurring during bacteriophage therapy. Viruses 10.

12. Oechslin F, Piccardi P, Mancini S, Gabard J, Moreillon P, Entenza JM, Resch G, Que YA. 2017. Synergistic interaction between phage therapy and antibiotics clears Pseudomonas Aeruginosa infection in endocarditis and reduces virulence. J Infect Dis 215:703–712.

13. Schooley RT, Biswas B, Gill JJ, Hernandez-Morales A, Lancaster J, Lessor L, Barr JJ, Reed SL, Rohwer F, Benler S, Segall AM, Taplitz R, Smith DM, Kerr K, Kumaraswamy M, Nizet V, Lin L, McCauley MD, Strathdee SA, Benson CA, Pope RK, Leroux BM, Picel AC, Mateczun AJ, Cilwa KE, Regeimbal JM, Estrella LA, Wolfe DM, Henry MS, Quinones J, Salka S, Bishop-Lilly KA, Young R, Hamilton T. 2017. Development and use of personalized bacteriophage-based therapeutic cocktails to treat a patient with a disseminated resistant Acinetobacter baumannii infection. Antimicrob Agents Chemother 61.

14. Yerushalmy O, Khalifa L, Gold N, Rakov C, Alkalay-Oren S, Adler K, Ben-Porat S, Kraitman R, Gronovich N, Ginat KS, Abdalrhman M, Coppenhagen-Glazer S, Nir-Paz R, Hazan R. 2020. The israeli phage bank (IPB). Antibiotics 9:1–7.

15. Nagel T, Musila L, Muthoni M, Nikolich M, Nakavuma JL, Clokie MR. 2022. Phage banks as potential tools to rapidly and cost-effectively manage antimicrobial resistance in the developing world. Curr Opin Virol 53:101208.

16. Savalia D, Westblade LF, Goel M, Florens L, Kemp P, Akulenko N, Pavlova O, Padovan JC, Chait BT, Washburn MP, Ackermann HW, Mushegian A, Gabisonia T, Molineux I, Severinov K. 2008. Genomic and Proteomic Analysis of phiEco32, a Novel Escherichia coli Bacteriophage. J Mol Biol 377:774–789.

17. Mirzaei MK, Eriksson H, Kasuga K, Haggård-Ljungquist E, Nilsson AS. 2014. Genomic, proteomic, morphological, and phylogenetic analyses of vB-EcoP-SU10, a *Podoviridae* phage with C3 morphology. PLoS One 9:1–19.

18. Koonjan S, Cooper CJ, Nilsson AS. 2021. Complete genome sequence of vb_ecop_su7, a *Podoviridae* coliphage with the rare c3 morphotype. Microorganisms 9:1–11.

19. Terwilliger A, Clark J, Karris M, Hernandez-Santos H, Green S, Aslam S, Maresso A. 2021. Phage therapy related microbial succession associated with successful clinical outcome for a recurrent urinary tract infection. Viruses 13.

20. Federici S, Kredo-Russo S, Valdés-Mas R, Kviatcovsky D, Weinstock E, Matiuhin Y, Silberberg Y, Atarashi K, Furuichi M, Oka A, Liu B, Fibelman M, Weiner IN, Khabra E, Cullin N, Ben-Yishai N, Inbar D, Ben-David H, Nicenboim J, Kowalsman N, Lieb W, Kario E, Cohen T, Geffen YF, Zelcbuch L, Cohen A, Rappo U, Gahali-Sass I, Golembo M, Lev V, Dori-Bachash M, Shapiro H, Moresi C, Cuevas-Sierra A, Mohapatra G, Kern L, Zheng D, Nobs SP, Suez J, Stettner N, Harmelin A, Zak N, Puttagunta S, Bassan M, Honda K, Sokol H, Bang C, Franke A, Schramm C, Maharshak N, Sartor RB, Sorek R, Elinav E. 2022. Targeted suppression of human IBD-associated gut microbiota commensals by phage consortia for treatment of intestinal inflammation. Cell 185:2879-2898.e24.

21. Anand T, Bera BC, Vaid RK, Barua S, Riyesh T, Virmani N, Hussain M, Singh RK, Tripathi BN. 2016. Abundance of antibiotic resistance genes in environmental bacteriophages. J Gen Virol 97:3458–3466.

22. Gómez-Gómez C, Blanco-Picazo P, Brown-Jaque M, Quirós P, Rodríguez-Rubio L, Cerdà-Cuellar M, Muniesa M. 2019. Infectious phage particles packaging antibiotic resistance genes found in meat products and chicken feces. Sci Rep 9:1–11.

23. Kohei K, Mitsuoki K, Motoyuki S, Mariana C. 2021. Distribution of Antimicrobial Resistance and Virulence Genes within the Prophage-Associated Regions in Nosocomial Pathogens. mSphere 0:e00452-21.

24. Haines MEK, Hodges FE, Nale JY, Mahony J, van Sinderen D, Kaczorowska J, Alrashid B, Akter M, Brown N, Sauvageau D, Sicheritz-Pontén T, Thanki AM, Millard AD, Galyov EE, Clokie MRJ. 2021. Analysis of Selection Methods to Develop Novel Phage Therapy Cocktails Against Antimicrobial Resistant Clinical Isolates of Bacteria. Front Microbiol 12:1–15.

25. Molina F, Simancas A, Ramírez M, Tabla R, Roa I, Rebollo JE. 2021. A New Pipeline for Designing Phage Cocktails Based on Phage-Bacteria Infection Networks. Front Microbiol 12:1–14.

26. Molina F, Flores MM, Fernández L, Rodríguez MAV. 2022. Systematic analysis of putative phage - phage interactions on minimum - sized phage cocktails. Sci Rep 1–12.

506 27. Tanji Y, Shimada T, Yoichi M, Miyanaga K, Hori K, Unno H. 2004. Toward rational control of
507 Escherichia coli O157:H7 by a phage cocktail. Appl Microbiol Biotechnol 64:270–274.
508 28. Hesse S, Rajaure M, Wall E, Johnson J, Bliskovsky V, Gottesman S. 2020. Phage Resistance in
509 Multidrug-Resistant Klebsiella pneumoniae ST258 Evolves via Diverse Mutations That Culminate in
510 Impaired Adsorption. MBio 11:1–14.
511 29. Gordillo Altamirano FL, Barr JJ. 2021. Unlocking the next generation of phage therapy: the key is in
512 the receptors. Curr Opin Biotechnol 68:115–123.
513 30. Olszak T, Shneider MM, Latka A, Maciejewska B, Browning C, Sycheva L V., Cornelissen A, Danis-
514 Wlodarczyk K, Senchenkova SN, Shashkov AS, Gula G, Arabski M, Wasik S, Miroshnikov KA,
515 Lavigne R, Leiman PG, Knirel YA, Drulis-Kawa Z. 2017. The O-specific polysaccharide lyase from
516 the phage LKA1 tailspike reduces Pseudomonas virulence. Sci Rep 7:1–14.
517 31. Hao G, Shu R, Ding L, Chen X, Miao Y, Wu J, Zhou H, Wang H. 2021. Bacteriophage SRD2021
518 recognizing capsular polysaccharide shows therapeutic potential in serotype K47 Klebsiella
519 pneumoniae infections. Antibiotics 10.
520 32. Chegini Z, Khoshbayan A, Taati Moghadam M, Farahani I, Jazireian P, Shariati A. 2020.
521 Bacteriophage therapy against Pseudomonas aeruginosa biofilms: A review. Ann Clin Microbiol
522 Antimicrob 19:1–17.

523 33. Liao Y-T, Zhang Y, Salvador A, Harden LA, Wu VCH. 2022. Characterization of a T4-like
524 Bacteriophage vB_EcoM-Sa45lw as a Potential Biocontrol Agent for Shiga Toxin-Producing
525 Escherichia coli O45 Contaminated on Mung Bean Seeds. Microbiol Spectr 10.
526 34. Ye N, Nemoto N. 2004. Processing of the tail lysozyme (gp5) of bacteriophage T4. J Bacteriol
527 186:6335–6339.
528 35. Burmeister AR, Fortier A, Roush C, Lessing AJ, Bender RG, Barahman R, Grant R, Chan BK, Turner
529 PE. 2020. Pleiotropy complicates a trade-off between phage resistance and antibiotic resistance. Proc
530 Natl Acad Sci U S A 117.
531 36. Gurney J, Pradier L, Griffin JS, Gougat-Barbera C, Chan BK, Turner PE, Kaltz O, Hochberg ME.
532 2020. Phage steering of antibiotic-resistance evolution in the bacterial pathogen, Pseudomonas
533 aeruginosa. Evol Med Public Heal 2020:148–157.
534 37. Liu CG, Green SI, Min L, Clark JR, Salazar KC, Terwilliger AL, Kaplan HB, Trautner BW, Ramig
535 RF, Maresso AW. 2020. Phage-antibiotic synergy is driven by a unique combination of antibacterial
536 mechanism of action and stoichiometry. MBio 11:1–19.
537 38. Nakamura K, Fujiki J, Nakamura T, Furusawa T, Gondaira S, Usui M, Higuchi H, Tamura Y, Iwano
538 H. 2021. Fluctuating Bacteriophage-induced galU Deficiency Region is Involved in Trade-off Effects
539 on the Phage and Fluoroquinolone Sensitivity in Pseudomonas aeruginosa. Virus Res 306:198596.

39. Roach DR, Donovan DM. 2015. Antimicrobial bacteriophage-derived proteins and therapeutic applications. Bacteriophage 5:e1062590.

40. Uchiyama J, Rashel M, Maeda Y, Takemura I, Sugihara S, Akechi K, Muraoka A, Wakiguchi H, Matsuzaki S. 2008. Isolation and characterization of a novel Enterococcus faecalis bacteriophage φEF24C as a therapeutic candidate. FEMS Microbiol Lett 278:200–206.

41. Kitamura N, Sasabe E, Matsuzaki S, Daibata M, Yamamoto T. 2020. Characterization of two newly isolated Staphylococcus aureus bacteriophages from Japan belonging to the genus Silviavirus. Arch Virol 165:2355–2359.

42. Seemann T. 2014. Prokka: Rapid prokaryotic genome annotation. Bioinformatics 30:2068–2069.

43. Tatusova T, Dicuccio M, Badretdin A, Chetvernin V, Nawrocki P, Zaslavsky L, Lomsadze A, Pruitt KD, Borodovsky M, Ostell J. 2016. NCBI prokaryotic genome annotation pipeline 44:6614–6624.

44. Altschul SF, Gish W, Miller W, Myers EW, Lipman DJ. 1990. Basic local alignment search tool. J Mol Biol 215:403–410.

45. Pritchard L, Glover RH, Humphris S, Elphinstone JG, Toth IK. 2016. Genomics and taxonomy in diagnostics for food security: Soft-rotting enterobacterial plant pathogens. Anal Methods 8:12–24.

555 46. Zankari E, Hasman H, Cosentino S, Vestergaard M, Rasmussen S, Lund O, Aarestrup FM, Larsen
556 MV. 2012. Identification of acquired antimicrobial resistance genes. J Antimicrob Chemother
557 67:2640–2644.
558 47. Chen L, Zheng D, Liu B, Yang J, Jin Q. 2016. VFDB 2016: Hierarchical and refined dataset for big
559 data analysis - 10 years on. Nucleic Acids Res 44:D694–D697.
560 48. Garneau JR, Legrand V, Marbouty M, Press MO, Vik DR, Fortier LC, Sullivan MB, Bikard D, Monot
561 M. 2021. High-throughput identification of viral termini and packaging mechanisms in virome
562 datasets using PhageTermVirome. Sci Rep 11:1–9.
563 49. Chan PP, Lin BY, Mak AJ, Lowe TM. 2021. TRNAscan-SE 2.0: Improved detection and functional
564 classification of transfer RNA genes. Nucleic Acids Res 49:9077–9096.
565 50. Page AJ, Taylor B, Delaney AJ, Soares J, Seemann T, Keane JA, Harris SR. 2016. SNP-sites: rapid
566 efficient extraction of SNPs from multi-FASTA alignments. Microb genomics 2:e000056.
567

568 **Figure Legends**

569 Fig. 1 Transmission electron microscopy images of 29 isolated phages. Each sample was
570 negatively stained and magnified at ×50,000. øKp_1 and øKp_22 are shown as
571 representative *Tevenviridae*. All *Podoviridae* and *Siphoviridae* are shown. The bar
572 represents 200 nm in individual images.

573

574 Fig. 2 Heatmap of the host range in each phage. X and Y axes represent phages and host
575 strains, respectively. *Klebsiella pneumoniae* ATCC BAA 1705 and ATCC BAA
576 1706 were used as standard strains, and *Escherichia coli* SK191 and BL21 were used
577 as control strains. The color in the heatmap represents the EOP. Bar charts on the X-
578 and Y-axes represent the number of infections in each phage and host, respectively.

579

580 Fig. 3 OD_{600} kinetics indicator bacteria incubated with phage. Bacterial strains were
581 incubated up to OD_{600} = 0.1, following which each phage was added at 10^9 pfu/ml.
582 OD_{600} was monitored at appropriate times until 24 h. No phage was added in Kp21
583 and Kp22 for the negative control. All experiments in this section were performed in
584 triplicate.

585 Fig. 4 Cocktail experiment of Kp21r and Kp22r. Phage-resistant Kp21 (Kp21r) and Kp22
586 (Kp22r) were derived from the culture medium after 24 h incubation with øKp_21 or
587 øKp_22. The cocktail consisted of 10 phages, and each phage was at 10^7 pfu/ml.
588 OD_{600} was monitored at appropriate times until 24 h. All experiments in this section
589 were performed in triplicate.
590
591 Fig. 5 Analysis of the shifting in susceptibility to the phage cocktail in f22 and f22r. (A) the
592 host range in f22 and f22r was investigated against 10 phages comprising a phage
593 cocktail. “S” represents a sparse bacterial lawn. (B) Colony forming units are
594 mentioned under each phage. f22 or f22r were mixed with individual phages, and 2 h
595 after phage addition, samples were diluted to 10^{-2} and 10^{-4}, and lawned onto LB
596 plates. n.d. means that colonies were not detected at the 10^{-2} condition.
597
598 Fig. 6 Characterization of phage-resistant Kp21r strain. (A) Adsorption assay of øKp_21
599 against Kp21 and Kp21r strains. Kp21 and Kp21r were incubated until OD_{600} = 0.5,
600 following which øKp_21 was added at 10^7 pfu/ml and incubated at 37°C with
601 shaking at 200 rpm. After 5 min, 200 µl of the mixture was withdrawn and

602 centrifuged at 9,100 ×*g* for 1 min. The number of phages in the supernatant was
603 measured. (B) 1.0×10^9 pfu of øKp_21 was mixed with 100 µl of overnight Kp21 or
604 Kp21r culture. Thereafter, 5 ml of 0.6 % soft agar was added to the host and phage
605 mixture and incubated at 37°C overnight. n.d. means that plaques were not detected.
606 (C) Nucleotide sequences of *cpsA* in Kp21 and Kp21r were aligned using ClustalW
607 (http://clustalw.ddbj.nig.ac.jp/). Insertion mutation (A) is shown by an arrow, and the
608 stop codons of *cspA* in f22 and f22r are shown by a square.
609
610
611
612 Fig. S1 All TEM images of *Myoviridae* in this study. The bar represents 200 nm in
613 individual images.
614
615 Fig. S2 Correlation between plaque size and EOP. Plaque size (mm^2) and EOP in the
616 phages were measured in representative phage strains. The X- and Y-axes show the
617 EOP in each phage and plaque size, respectively. A maximum of 10 plaques were
618 randomly selected in individual phage-host combinations and plaque sizes were

619 measured using ImageJ. Python packaging Seaborn was used to visualize the
620 correlation, and R correlation in each combination was calculated using Scipy
621 version 1. 8. 1.
622
623 **Tables**
624 Table S1 The genomic information of phages isolated in Japan. Genome assembly was
625 performed using Shovill with default settings. Phage contigs were filtered with the
626 contig length < 200 and/or coverage < 25. “CDS after filtered” and “contigd_filtered”
627 columns represent the number of CDS from the filtered contigs. The packaging
628 mechanism and terminal repeats in each phage were presumed using
629 Phagetermvirome.
630
631 Table S2 The table of host range and EOP for all host-phage combination. EOP was
632 calculated by plaques of individual phage and host combination divided by plaques
633 of indicator host and phage combination.
634

635 Table S3 The list of the domain prediction for each phage protein. Pfam-A 27 was used as

636 phage database.

637

638 Table S4 The list of SNPs between Kp21 and Kp21r. SNPs were detected using Snippy as

639 default settings.

Fig. 1

øEc_1

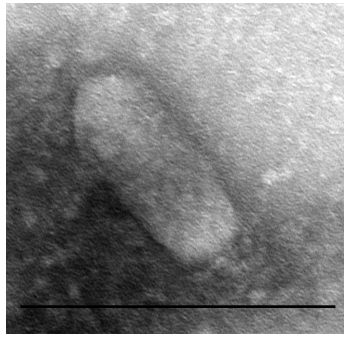

øKp_30

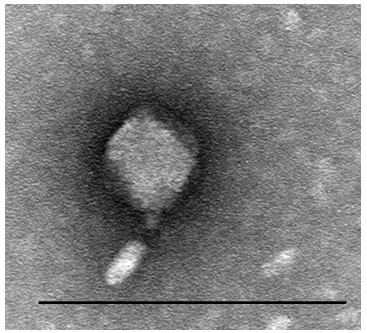

øKp_31

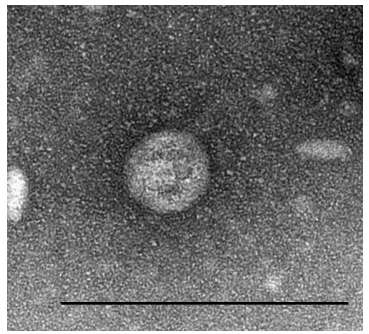

øKp_7-1

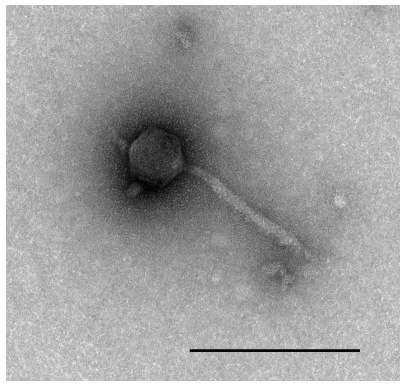

øKp_7-2

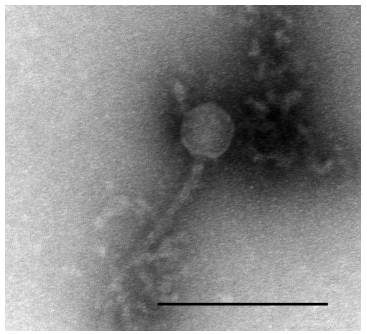

øKp_14

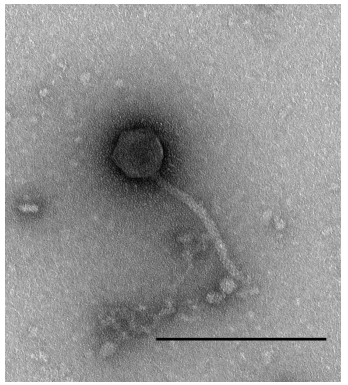

øKp_24

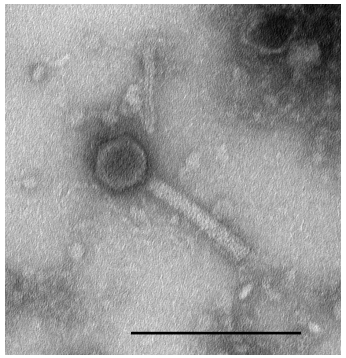

øKp_27

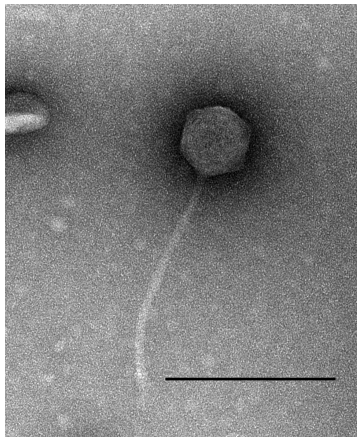

øKp_1

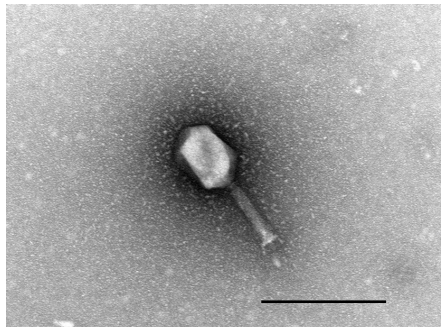

øKp_21

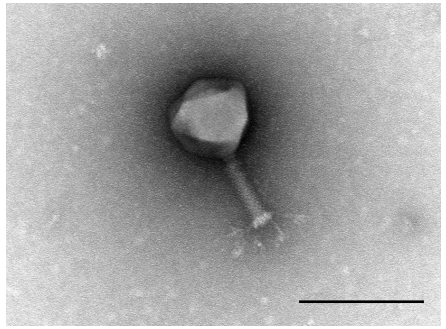

øKp_22

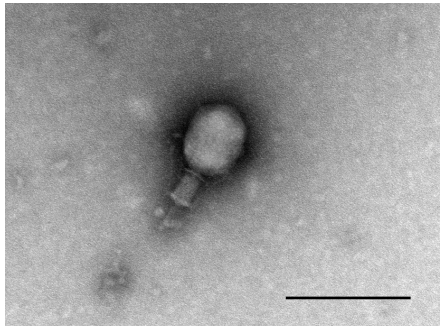

øKp_32

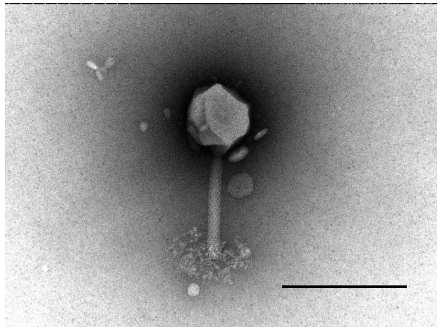

Fig. 2

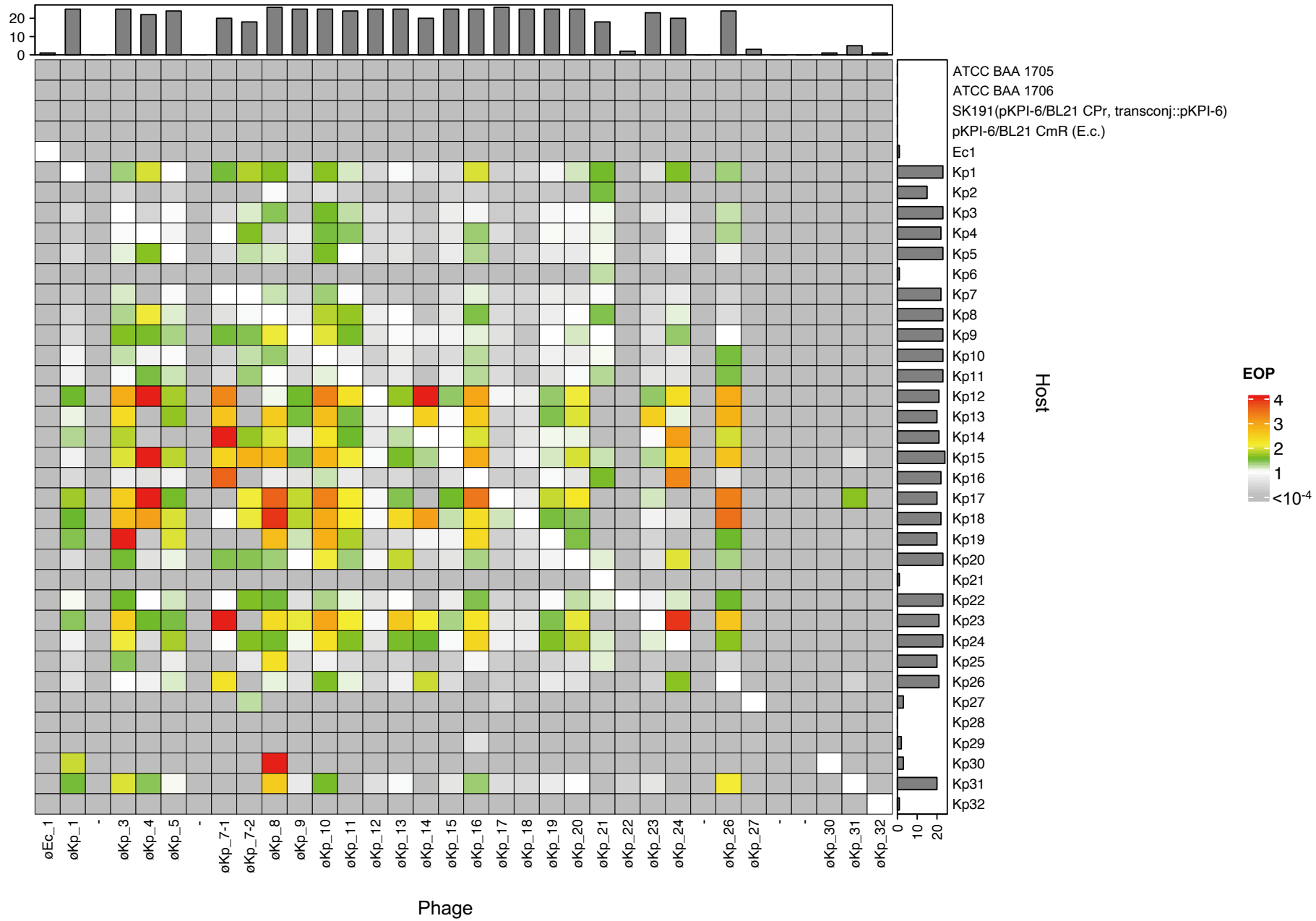
20
10
0
ATCC BAA 1705
ATCC BAA 1706
SK191(pKPI-6/BL21 CPr, transconj::pKPI-6)
pKPI-6/BL21 CmR (E.c.)
Ec1
Kp1
Kp2
Kp3
Kp4
Kp5
Kp6
Kp7
Kp8
Kp9
Kp10
Kp11
Kp12
Kp13
Kp14
Kp15
Kp16
Kp17
Kp18
Kp19
Kp20
Kp21
Kp22
Kp23
Kp24
Kp25
Kp26
Kp27
Kp28
Kp29
Kp30
Kp31
Kp32
Host
EOP
4
3
2
1
<10-4
øEc_1
øKp_1
-
øKp_3
øKp_4
øKp_5
-
øKp_7-1
øKp_7-2
øKp_8
øKp_9
øKp_10
øKp_11
øKp_12
øKp_13
øKp_14
øKp_15
øKp_16
øKp_17
øKp_18
øKp_19
øKp_20
øKp_21
øKp_22
øKp_23
øKp_24
-
øKp_26
øKp_27
-
-
øKp_30
øKp_31
øKp_32
0
10
20
Phage

Fig. 3

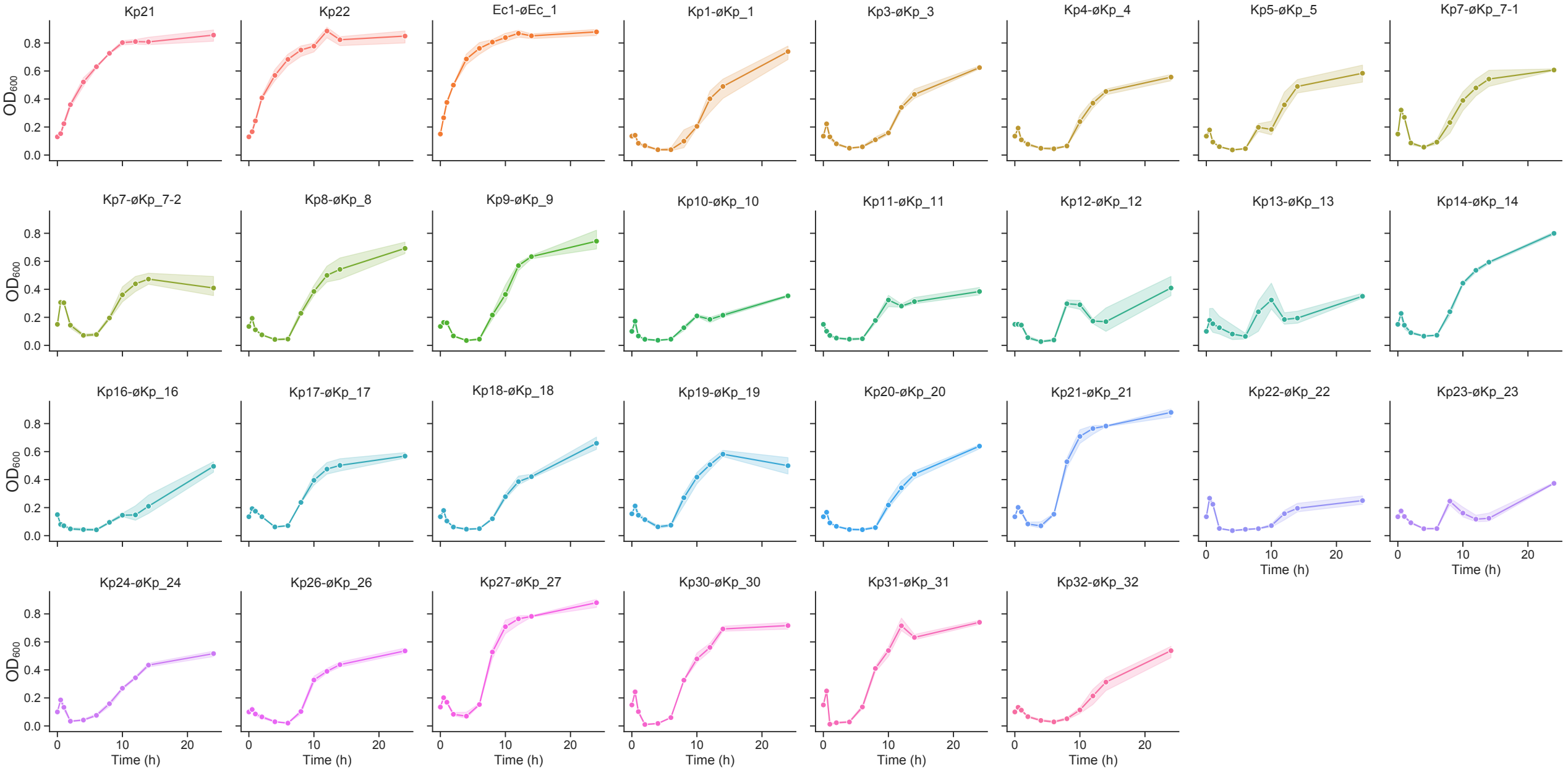
Kp21
Kp22
Ec1-øEc_1
Kp1-øKp_1
Kp3-øKp_3
Kp4-øKp_4
Kp5-øKp_5
Kp7-øKp_7-1
Kp7-øKp_7-2
Kp8-øKp_8
Kp9-øKp_9
Kp10-øKp_10
Kp11-øKp_11
Kp12-øKp_12
Kp13-øKp_13
Kp14-øKp_14
Kp16-øKp_16
Kp17-øKp_17
Kp18-øKp_18
Kp19-øKp_19
Kp20-øKp_20
Kp21-øKp_21
Kp22-øKp_22
Kp23-øKp_23
Kp24-øKp_24
Kp26-øKp_26
Kp27-øKp_27
Kp30-øKp_30
Kp31-øKp_31
Kp32-øKp_32
OD600
Time (h)
0.0
0.2
0.4
0.6
0.8
0
10
20

Fig. 4

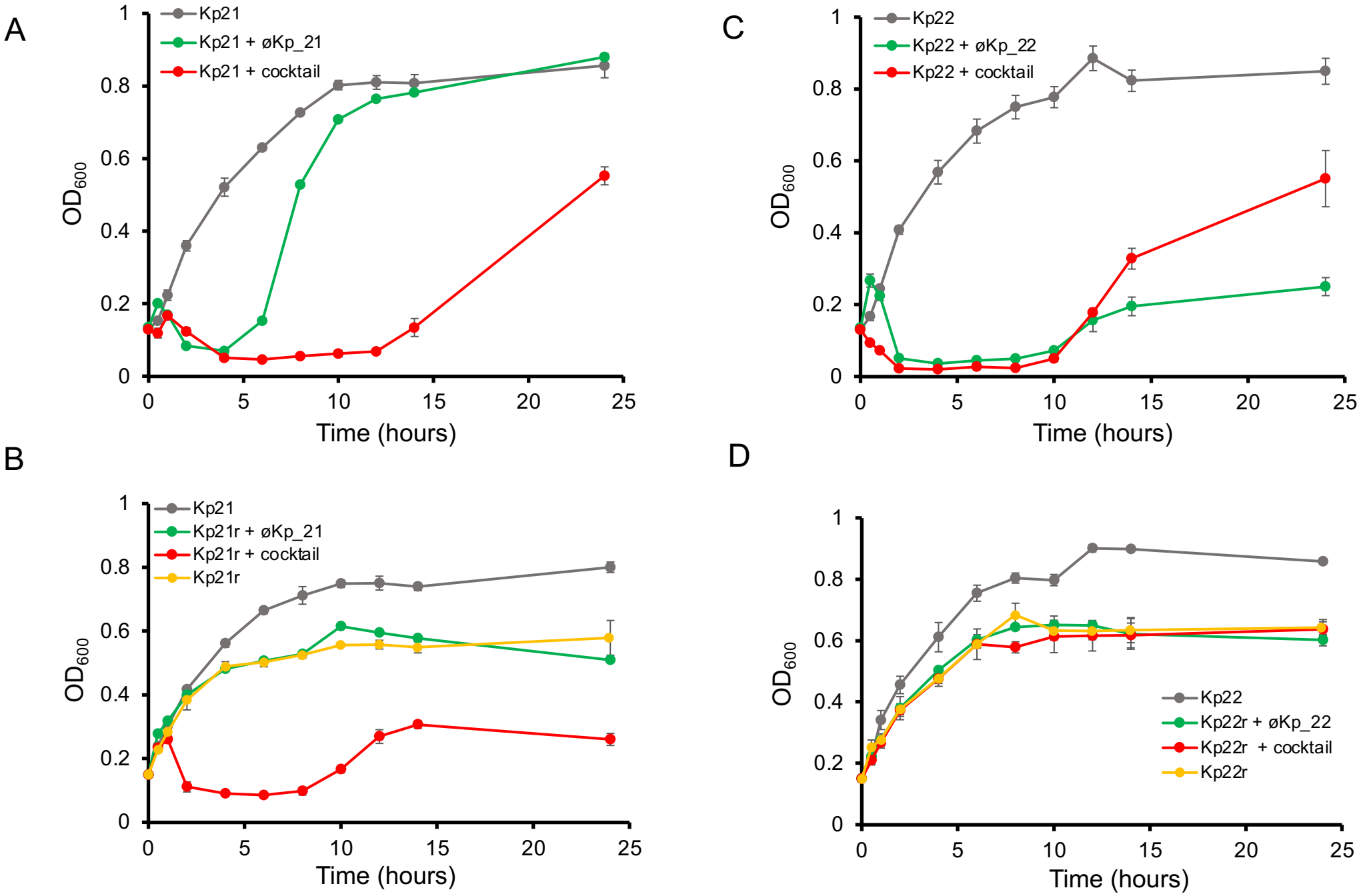
A
Kp21
Kp21 + øKp_21
Kp21 + cocktail
OD600
Time (hours)
B
Kp21
Kp21r + øKp_21
Kp21r + cocktail
Kp21r
OD600
Time (hours)
C
Kp22
Kp22 + øKp_22
Kp22 + cocktail
OD600
Time (hours)
D
Kp22
Kp22r + øKp_22
Kp22r + cocktail
Kp22r
OD600
Time (hours)

Fig. 5

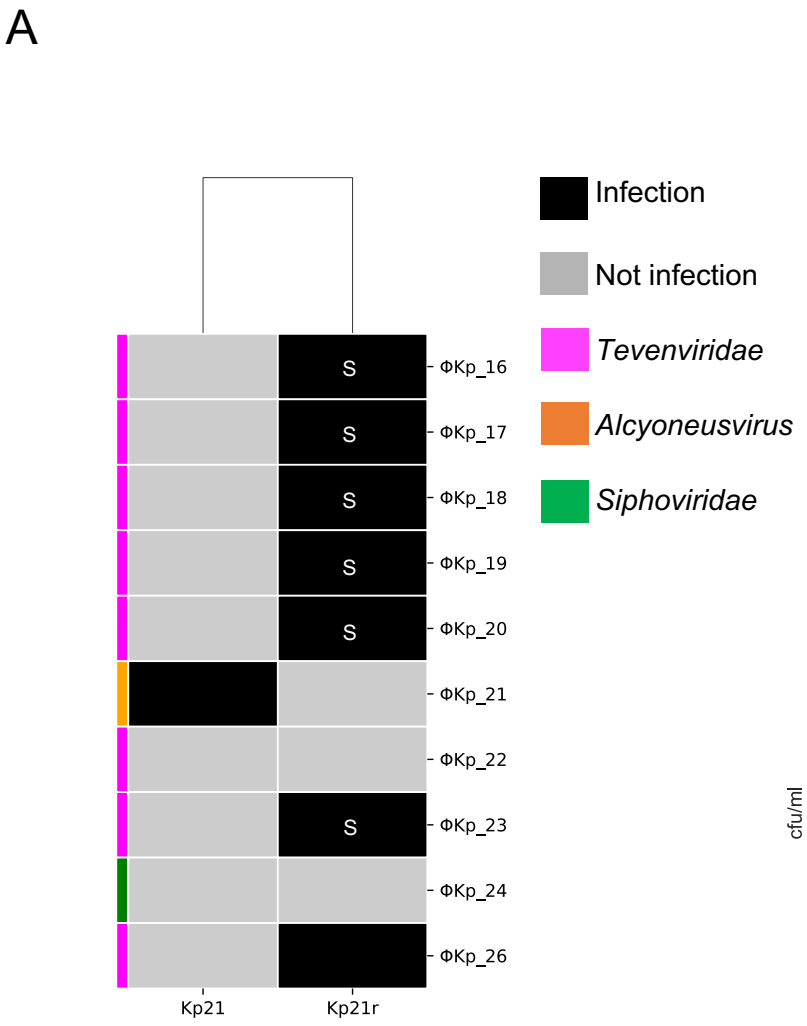
A
S
ΦKp_16
ΦKp_17
ΦKp_18
ΦKp_19
ΦKp_20
ΦKp_21
ΦKp_22
ΦKp_23
ΦKp_24
ΦKp_26
Kp21
Kp21r
Infection
Not infection
Tevenviridae
Alcyoneusvirus
Siphoviridae

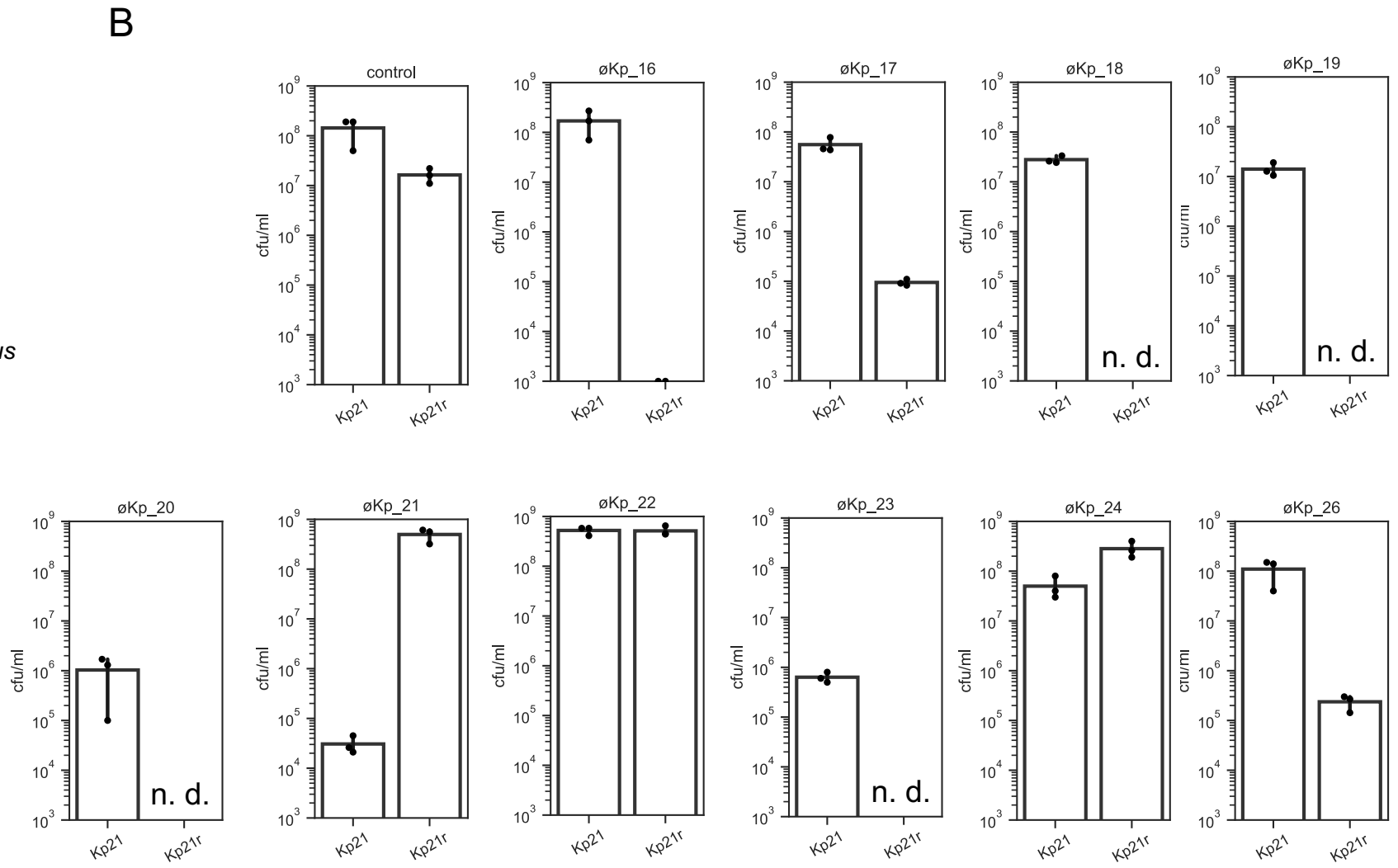
B
control
øKp_16
øKp_17
øKp_18
øKp_19
øKp_20
øKp_21
øKp_22
øKp_23
øKp_24
øKp_26
cfu/ml
Kp21
Kp21r
n. d.

Fig. 6

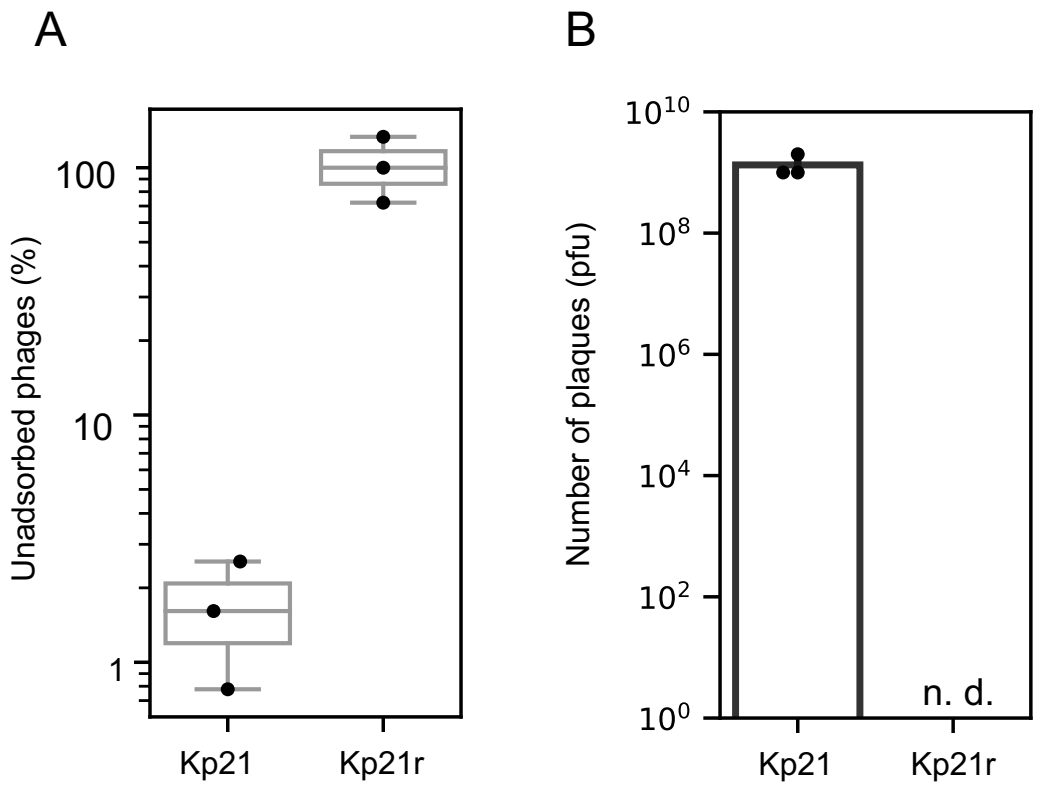

C

```
Kp21_cpsA  ATGCAATATT TTTTTGTTAA AGTTTTAAAA AAACTAAGTG CCTTTTTTAG AATAAAATTC TTATCCGATT TGTATAAAAA 80
Kp21r_cpsA ATGCAATATT TTTTTGTTAA AGTTTTAAAA AAACTAAGTG CCTTTTTTAG AATAAAATTC TTATCCGATT TGTATAAAAA 80

Kp21_cpsA  TGTTTTTTTG TTTTTTTTGG ATAAAAGTAT TGGCAGCCCA GATTATGAAA AATACAATCA TCTTAGTGAA GATAGTATAA 160
Kp21r_cpsA TGTTTTTTTG TTTTTTTTGG ATAAAAGTAT TGGCAGCCCA GATTATGAAA AATACAATCA TCTTAGTGAA GATAGTATAA 160

Kp21_cpsA  TAAATCGAAC TATTTGGGTT TATTGGGCCC AAGGATTAGA TAATGCACCT CCAGTAGTTC AGAATTGTGT CAAAACTCTC 240
Kp21r_cpsA TAAATCGAAC TATTTGGGTT TATTGGGCCC AAGGATTAGA TAATGCACCT CCAGTAGTTC AGAATTGTGT CAAAACTCTC 240

Kp21_cpsA  AAAGAGAATT CATCTCCAGA TTTTGTAGTA CAGGTGGTTG ATGATTTTAA TTTGGTTGAT TATATTGATA TACCAGAGAT 320
Kp21r_cpsA AAAGAGAATT CATCTCCAGA TTTTGTAGTA CAGGTGGTTG ATGATTTTAA TTTGGTTGAT TATATTGATA TACCAGAGAT 320

Kp21_cpsA  TATTAATACC AGATTAAAAG AGGGAGTAAT CTCGCGTACA CACTTTAGTG ATATTGTTAG ATTTGAATTA TTAAAAAAGC 400
Kp21r_cpsA TATTAATACC AGATTAAAAG AGGGAGTAAT CTCGCGTACA CACTTTAGTG ATATTGTTAG ATTTGAATTA TTAAAAAAGC 400

Kp21_cpsA  ATGGCGGAGT CTGGATTGAT AGTACAGTAT TGGTTGCTGA GAACTTTAGG G▼GGGTTTTA AATAAATTCT CAAAATTTAT 479
Kp21r_cpsA ATGGCGGAGT CTGGATTGAT AGTACAGTAT TGGTTGCTGA GAACTTTAGG GAGGGTTTTA AATAAATTCT CAAAATTTAT 480

Kp21_cpsA  TACATTGAAC CATAATGATC ATAACCCTTA TACTGCAATA ACCGAAGGCA GATGGACATC CTTCTTTATA GGCATGCCGA 559
Kp21r_cpsA TACATTGAAC CATAATGATC ATAACCCTTA TACTGCAATA ACCGAAGGCA GATGGACATC CTTCTTTATA GGCATGCCGA 560

Kp21_cpsA  AGCATTCCGC ACTTGCCGAT TTTATGTCGG ATGCATTTGT GTCCTATTGG AAAAAGAATA GCAAACTTAT AGACTATGTT 639
Kp21r_cpsA AGCATTCCGC ACTTGCCGAT TTTATGTCGG ATGCATTTGT GTCCTATTGG AAAAAGAATA GCAAACTTAT AGACTATGTT 640

Kp21_cpsA  CTTGTGGATT ATCTGATTGC CTTGGCTTAT AAGAAAATAC CAGCAGTACA AGAAATGATA ATTGGGCAAA ATGAGCTCAT 719
Kp21r_cpsA CTTGTGGATT ATCTGATTGC CTTGGCTTAT AAGAAAATAC CAGCAGTACA AGAAATGATA ATTGGGCAAA ATGAGCTCAT 720

Kp21_cpsA  TGGTAACTCT CGTTGGTTTC TACAAAAAGT TTATGATAAA AAAATATCTA TTGATATTGA TGAGGCAATA AATTCAGATA 799
Kp21r_cpsA TGGTAACTCT CGTTGGTTTC TACAAAAAGT TTATGATAAA AAAATATCTA TTGATATTGA TGAGGCAATA AATTCAGATA 800

Kp21_cpsA  TATATAAAAT TTATAAACTT ACTTATAAGC TAACTCCACC GATGGATAAG GATACCTATT ATTATAAGTT TTTTTGCCCT 879
Kp21r_cpsA TATATAAAAT TTATAAACTT ACTTATAAGC TAACTCCACC GATGGATAAG GATACCTATT ATTATAAGTT TTTTTGCCCT 880

Kp21_cpsA  GAGAAATGA 888
Kp21r_cpsA GAGAAATGA 889
```

Fig. S1

øKp_3

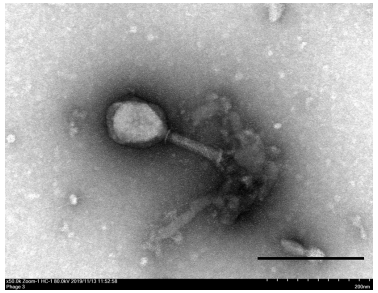

øKp_4

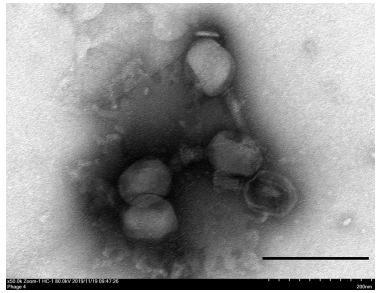

øKp_5

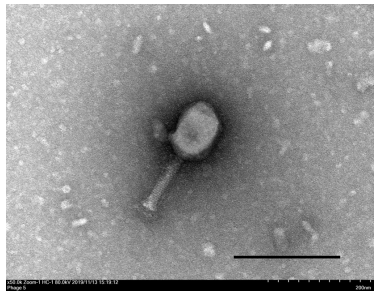

øKp_8

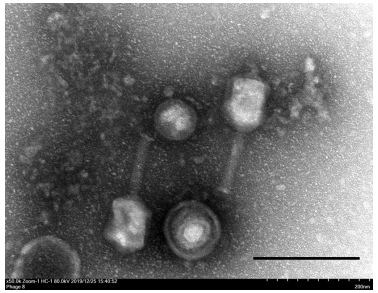

øKp_9

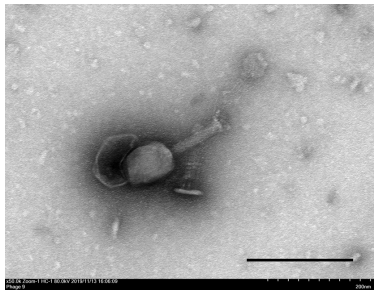

øKp_10

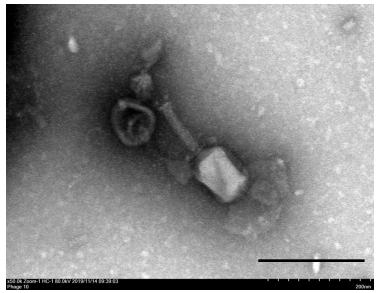

øKp_11

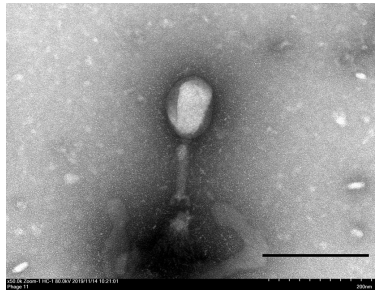

øKp_12

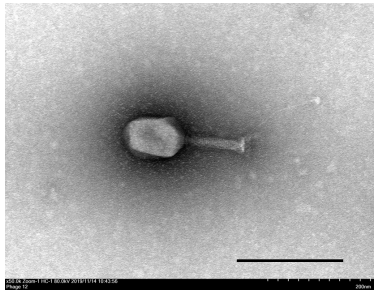

øKp_13

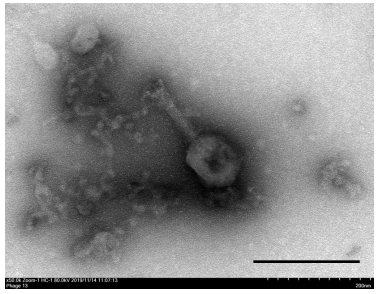

øKp_15

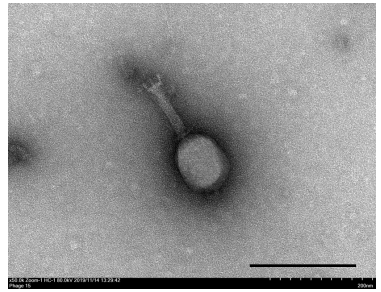

øKp_16

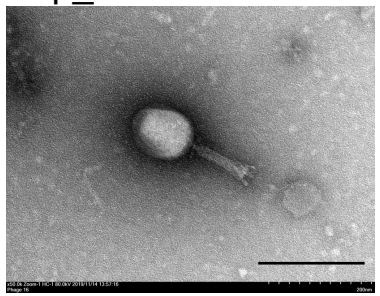

øKp_17

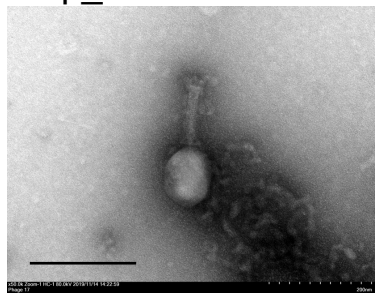

øKp_18

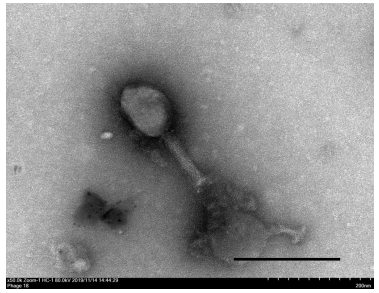

øKp_19

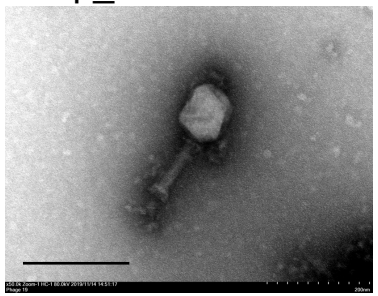

øKp_20

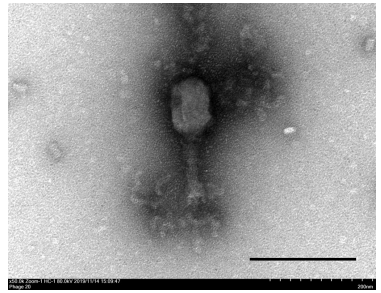

øKp_23

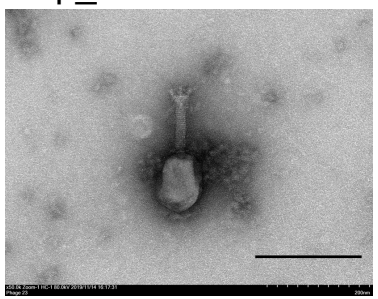

øKp_26

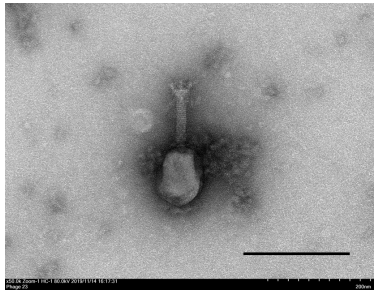

Fig. S2

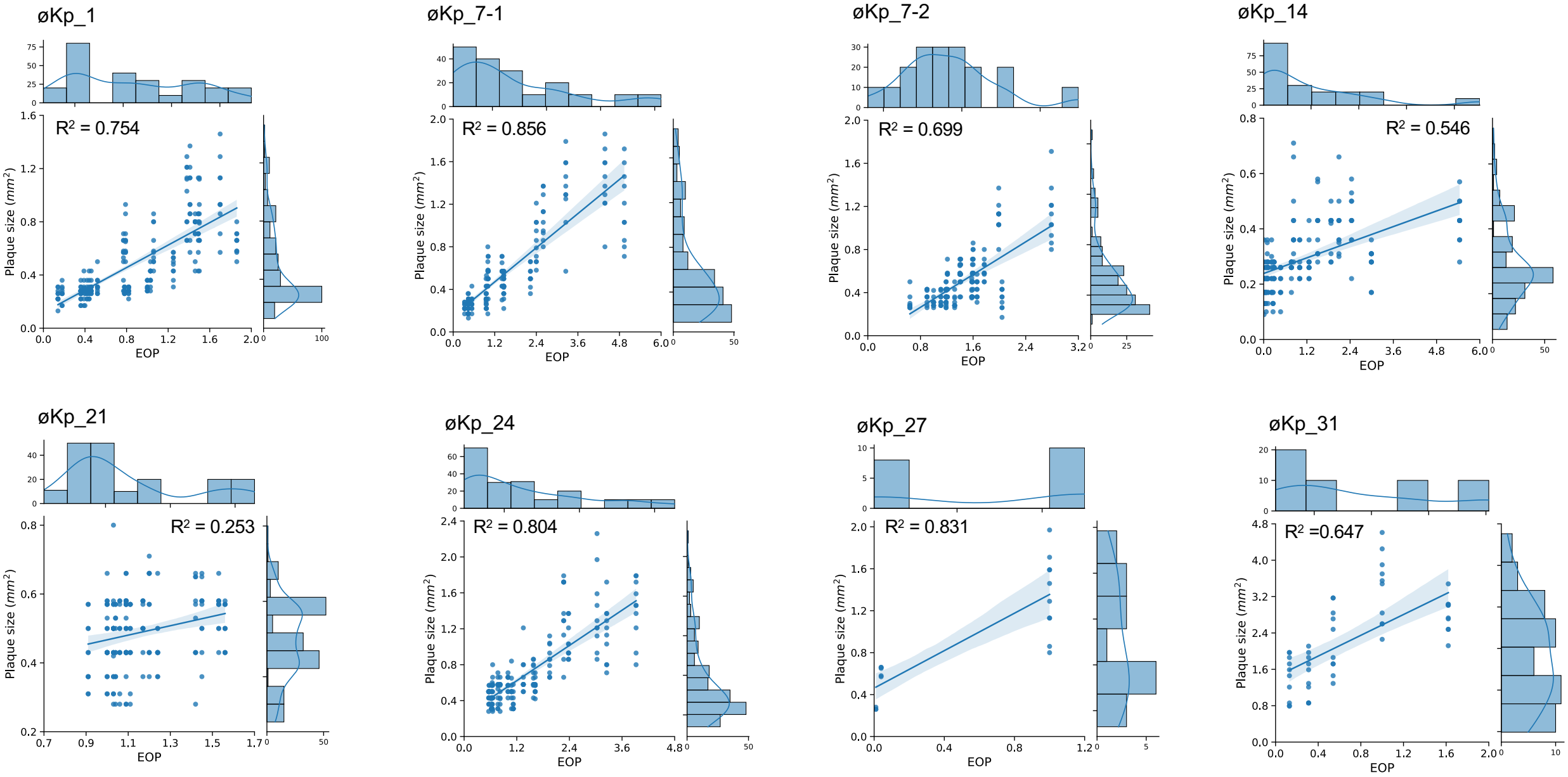
øKp_1
R² = 0.754
øKp_7-1
R² = 0.856
øKp_7-2
R² = 0.699
øKp_14
R² = 0.546
øKp_21
R² = 0.253
øKp_24
R² = 0.804
øKp_27
R² = 0.831
øKp_31
R² =0.647
Plaque size (mm^2)
EOP